CERN/ET Internal note 96-024

July, 9 1996

A Tungsten-Rhenium Alloy as a beam window material for the Energy Amplifier

S. Buono, A. Catinaccio, C. Rubbia

1.0 Introduction

In reference [1] we developed a detailed numerical model of the Energy Amplifier (EA) [2] using Star-CD [3] to show how the natural circulation of Lead can be an effective and safe way of implementing the primary cooling loop.

We used such a general model to evaluate the thermal and mechanical behaviour of the beam window under natural convection cooling. The beam window and the beam dump region were in fact accurately defined in the Star-CD model in order to give a full hydraulic description of the flow and a detailed thermal map in steady-state conditions.

The heat source map was accurately evaluated using Fluka [4], and successively inserted into the star-CD model.

Data extracted from the thermal hydraulic simulation were finally included in an ANSYS [5] model in order to evaluate the induced stresses, the creep behaviour and instability problems of the window under normal operating conditions.

In reference [6] we considered the use of Tungsten as a window material. Here we evaluated the use of a Tungsten-Rhenium (26%) alloy which, in addition to the favourable mechanical and physical properties of Tungsten (high thermal conductivity and melting point, small vapour pressure and, among all metals the smallest dilatation coefficient and the highest mechanical resistance), shows increased mechanical resistance, better workability and weldability, a higher recrystallization temperature, a lower brittle to ductile transition temperature, and a better resistance to void swelling under neutron irradiation and thermal creep.

2.0 Tungsten-Rhenium alloys properties

2.1 Physical and mechanical properties

Tungsten is one of the most promising structural materials to be used in high temperatures applications thanks to its outstanding characteristics:

- It has the highest melting point of all metals (3410 °C).
- It has a very high thermal conductivity, ensuring lower temperature differences in the beam window under irradiation and therefore, lower thermal induced stresses.
- It has, among all metals, the lowest dilatation coefficient, another important factor reducing thermal induced stresses and deformations.
- It has an excellent mechanical resistance at high temperature.
- It is not corroded by molten Lead [7].
- It has good activation properties (neutron absorptions and decays lead to stable Rhenium isotopes).
- It has a negligible vapour pressure.

The major limitations in the use of Tungsten for its application as a beam window material are its bad workability and weldability, the relatively rapid reductions of strengths at very high temperatures, the brittleness after recrystallization or under neutron irradiation.

Such limitations are overcome in many tungsten-base alloys that are being considered in many demanding fields, especially in space research [8] [9] and military applications [10].

The addition of Rhenium in a Tungsten based alloy, after a first softening effect up to 3.6 % Rhenium content (in weight), shows an important increase in the ultimate tensile strength (UTS) and tensile strength (TS) up to 30%, for a weight percent of 26 [11]. The addition of refractory oxides like ThO_2 (1 wt. %, not applicable in our case) or carbides like HfC (0.36 wt. %) further enhances the dispersion strengthening effect, until very high temperatures (2700 °K) as well as the creep strength [8]. In particular W-Re(26)-HfC(0.36) alloy is considered by far the strongest metallic material at temperatures above 2000 °K [11].

Pure Tungsten has a recrystallization temperature ranging from 1150 to 1350 °C [12]. The addition of Rhenium to Tungsten retards progressively the recrystallization or grain growth. In general, the greater the Re content, the higher is the recrystallization temperature [13] which, for W-Re(26), ranges from 1500 to 1650 °C [12]. For W-Re(4)-HfC(0.35) this temperature increases from 1800 to 1900 °C , thanks to the dragging effect of Hafnium Carbide particles on the recrystallization process.

Unalloyed Tungsten is brittle at ambient temperature and difficult to work, but it becomes ductile at elevated temperatures. The brittle-to-ductile transition

temperature depends on the degree of purity, the previous deformation, the annealing status and other factors, and can range from 200 to 500 °C, while for W-Re(26) it is about 90 °C.

When Tungsten is heated above the recrystallization temperature, its structure is altered due to grain growth which reduces strength and hardness and causes brittleness. This embrittlement process is absent in Tungsten-Rhenium alloys [12].

2.2 Radiation effects

The effect of radiation damage on material properties due to the spallation mechanism is still the most unknown argument because of the differences in the nuclear interactions with nuclear reactors and other radiation environments. Very little data on spallation induced radiation damage have been collected, given the relative novelty of this field and the limited power of the existing spallation facilities.

He production from (p, α) or (n, α) reactions, can be for example in steel, of the order of 200 appm/dpa in a spallation source, while it is just 10 appm/dpa in Fusion and 0.2 in Fast Fission reactors. Therefore Helium embrittlement seems to be the worse problem [14], since this gas has a strong tendency to precipitate into bubbles. The He/dpa ratio decreases with increasing atomic number, from about 400 for Al to 100 for W in the case of spallation [15]. Moreover, calculated estimates of He production can vary by a factor 10 using different tools and databases, hence an important experimental validation is needed.

Although Hydrogen production rate is about an order of magnitude higher than the Helium rate, this is not considered a problem, since Hydrogen diffuses so fast, especially at high temperatures, that only very small concentrations can build up.

Another problem that could play an important role in radiation damage is the production of solid impurities, not only for their effects on mechanical and physical properties, but also on corrosion by liquid Lead. Concerning neutron induced transmutation we do not expect significant changes in composition since subsequent neutron absorption in naturally occurring W or Re isotopes lead to other stable W or Re isotopes. This has also been experimentally verified in reference [16].

Swelling has also a relevant effect on mechanical properties as well as irradiation creep although this last effect is dominant over thermal creep only for temperatures less than about 500 °C. W-Re alloys with a Re composition of at least 10 at%, have showed a good resistance to void swelling, after irradiation under a fast neutron fluence of 4×10^{22} n cm^{-2} (E > 0.1 MeV) at temperature ranging from 575 to 675 °C, corresponding to a dose of 8.6 dpa [16]. The suppression of void swelling is probably due to the strong recombination process of self-interstitial atoms which prevents the accumulation of a sufficient number of vacancies for the nucleation and growth of voids. A confirmation of the suppression of void swelling in W-Re(25) alloys compared to pure W, is given in reference [17], where specimens of these materials have been exposed to a fast neutron fluence of 10^{22} n cm^{-2} (E > 1 MeV) at temperature ranging from 430 to 1000 °C, corresponding to a dose of about 9.5 dpa.

Neutron embrittlement is also an important factor. In the case of W-Re(25) the exposition of a specimen to 5.6×10^{20} fast neutrons (> 1 MeV) per cm^2 at room

temperature shows a strong strengthening effect (an increase of about 50% in the UTS) during a test at 1090 °C, but a substantial lost in material ductility [18]. Radiation hardening, which is generally accompanied by a reduction of the fracture toughness, i.e. the resistance of a material to crack propagation, saturates at displacement doses of around 10 dpa [15].

The ductile-to-brittle transition temperature (DBTT) is known to increase by irradiation. If the increase is large the material would always operate in a state of low fracture toughness. Irradiation of a W-Re (10) specimen under a fluence of 10^{24} n m^{-2} showed a DBTT shifts of only 31 °C, while it raised to > 900 °C for a fluence of 5.6 x 10^{25} n m^{-2} [19], corresponding to only 11 days of operation in the Energy Amplifier (average neutron flux in the window ~ $6x10^{19}$ n m^{-2} s^{-1}). Should this be the case also for W-Re(26), the beam window would operate, at a certain moment, in the brittle regime.

Neutron irradiation can have an influence also on the physical properties of the materials. It can cause, for example, a reduction of the thermal conductivity.

The utilisation of the structural material of the window at high temperature, although not desirable from the point of view of strength, could have an important effect in defect recovery from irradiation. It is anyway clear that an important experimental activity has to be started to determine the effects of a proton spallation induced radiation damage on the mechanical and physical properties of the structural material of the window.

3.0 Results of the analysis

3.1 Heat deposition by the particle beam (FLUKA)

The heat deposition in the hemispherical beam window (1.5 ÷ 3 mm variable thickness) by the 1 GeV proton beam, has been accurately calculated using FLUKA [4], and the results of this calculation have been successively inserted into the Star-CD model.

The beam size on the window was typically a circular spot of 15 cm diameter. In the Montecarlo calculations the beam distribution has been approximated with the parabola:

$$\frac{2I_o}{\pi r_o^2}\left(1-\frac{r^2}{r_o^2}\right)$$

With r_o = 7.5 cm and I_o =10 mA we have, for example, a peak current density of 113.2 $\mu A/cm^2$ in the centre of the window, corresponding to a heat flux of about 560 W/cm^2, considering that the energy loss by a proton at 1 GeV in Tungsten is about 24 MeV/cm, and that there is an important contribution of secondary particles heating from the Lead target.

Details of the heat flux distribution generated by the proton beam in the W-Re(26) window, are shown in figure 1.

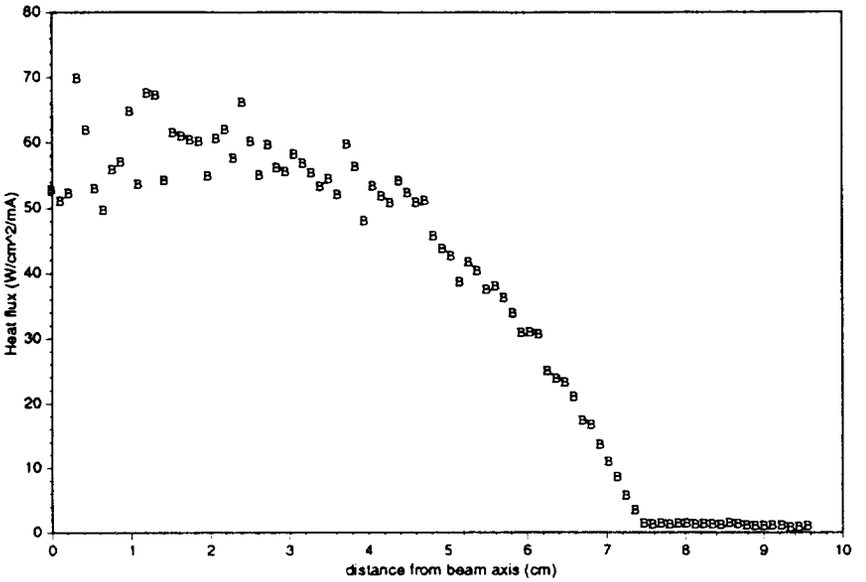

***Figure 1** - Heat flux generated in the window by a parabolic proton beam.*

Figure 2 shows the heat flux distribution generated by the proton beam for a uniformly distributed beam. This uniformity could be achieved by letting the beam pass through one or more diffusers, before hitting the window.

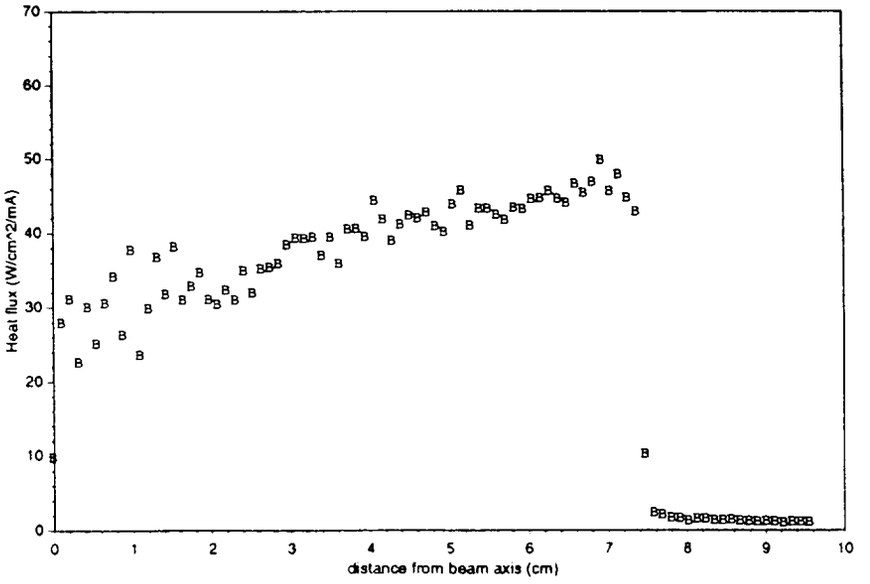

***Figure 2** - Heat flux generated in the window by a uniform proton beam.*

These results have been obtained from Fluka calculations with 50,000 protons. Beam intensities in the thermal hydraulic simulation covered a range from 10 to 20 mA.

3.2 The thermal hydraulic analysis (Star-CD)

Thanks to the lower flow resistance of the buffer region of the Energy Amplifier with respect to the core region, Lead average speed in the beam interaction zone is about 1.6 m/s, allowing an effective beam window cooling, although based on natural convection only.

The Lead speed in this region is principally due to the natural convection draft provoked by the core heating, and only in a very little extent to the convection induced by the beam heating itself. Doubling the beam intensity in fact, increases the Lead maximum speed by less than 1 %.

The maximum temperatures reached in the window and in the Lead dump region, as a function of beam intensity, for different beam profiles, are shown in figure 3.

We remark that, in case of a parabolic profile, the maximum temperature in the window is reached in the centre of the hemisphere, since, although the thickness traversed by the beam particles is smaller, the particle density is higher, not only in the window, but also in the Lead dump. Lead is therefore strongly heated in a region were its velocity is low, due to the presence of a theoretical stagnation point in the centre of the window.

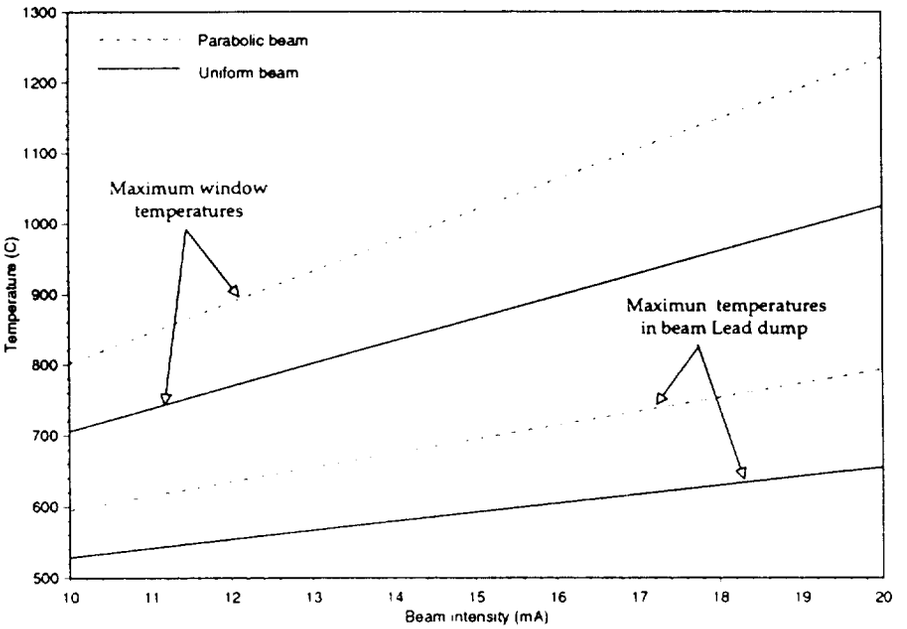

Figure 3 *- Maximum window and lead temperatures vs. beam intensity for different beam profiles.*

In case of a uniform beam, the situation is fairly different. The heat source is uniformly distributed and the Lead temperature in the region where its speed is lower is therefore also lower. The maximum temperature in the window is also lower, but it is reached at the edge of the beam spot, at about 45 degrees from the beam axis on the surface of the window, where the maximum thickness is traversed by the protons.

Since outside the beam spot the heating is absent, we have a higher thermal gradient, compared to the case of a parabolic profile, that could result in higher local stresses.

3.3 The structural analysis (ANSYS)

The window mesh created in star-CD was directly imported into an ANSYS model as well as the temperature maps obtained from the thermal hydraulic simulations, for different beam intensities (10 to 20 mA) and beam configurations (uniform or parabolic).

Stress behaviour

Figure 4 (at the end of the document) shows a typical stress map in the tangential direction of the beam window, for a beam intensity of 10 mA and a parabolic beam profile. The thermal gradient inside the window creates high thermal stresses inducing dilatation and deformation.

These stresses are distributed in the whole beam spot region, reaching their maximum value in the proximity of the centre of the window whose external fibres are in tension, while the internal are compressed.

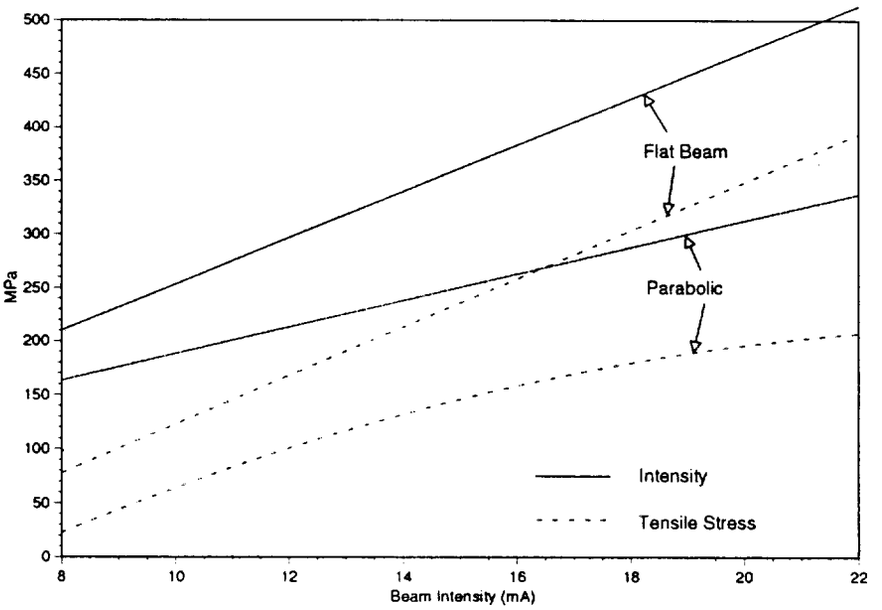

***Figure 6** - Maximum tensile and intensity stresses vs. beam intensity for different beam profiles.*

Figure 5 (at the end of the document) shows a typical stress map in the same conditions but with a flat beam profile. The situation is fairly different, since the maximum stress is not reached in the proximity of the centre of the window but on the edge of the beam spot, where the maximum heat is deposited. As we expected, being the thermal gradients higher, thermal stresses are also higher in this configuration.

In figure 6 we show a comparison between the maximum tensile and intensity stresses in the beam window as a function of the beam intensity[1], for different beam configurations.

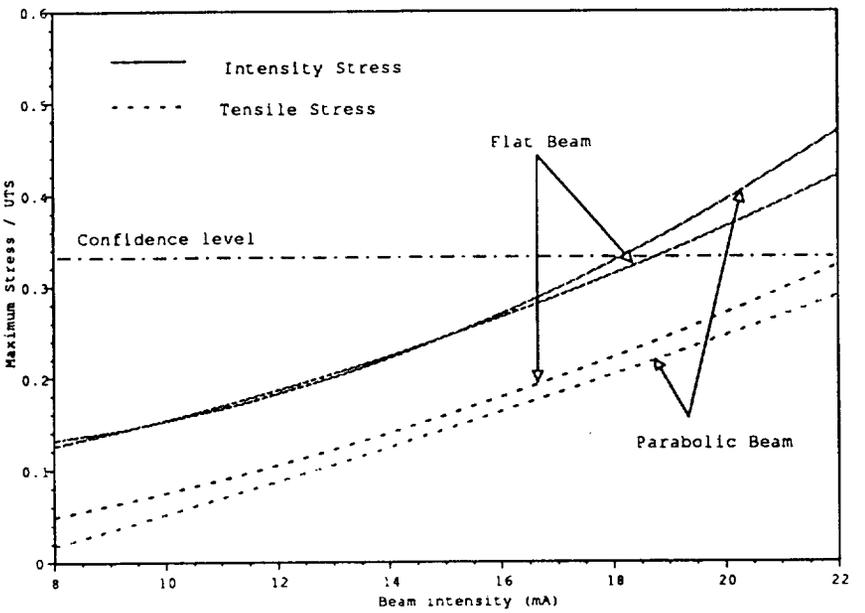

Figure 7 - Ratio between maximum Intensity or Tensile Stresses and UTS vs. beam intensity for different beam profiles.

In figure 7 we show the ratio between the stresses and the Ultimate Tensile Strength (UTS) of the material as found in ref. [20-22], showing that, in both configurations, the stresses overcome the confidence level at about 18 mA (if we consider the intensity stresses).

We can notice that, although in the flat configuration we have higher thermal stresses, the window is operated at lower temperature . This results in about the same safety margin in both configurations.

This margin must be considered a low limit, since in the reality the situation is slightly better. At high beam intensities in fact, the thermal creep induces a permanent deformation of the window that rapidly reduces the nominal stresses.

Creep behaviour

The phenomenon of creep becomes of engineering significance at homologous temperature $T_H = T/T_m$ greater than 0.5 (where T_m is the melting temperature). In the case of the beam window the maximum homologous temperature is reached at 20 mA in the centre of the hemisphere ($T_H = 0.4$).

---

[1] The intensity stress is the maximum value of the absolute differences between the principal stresses.

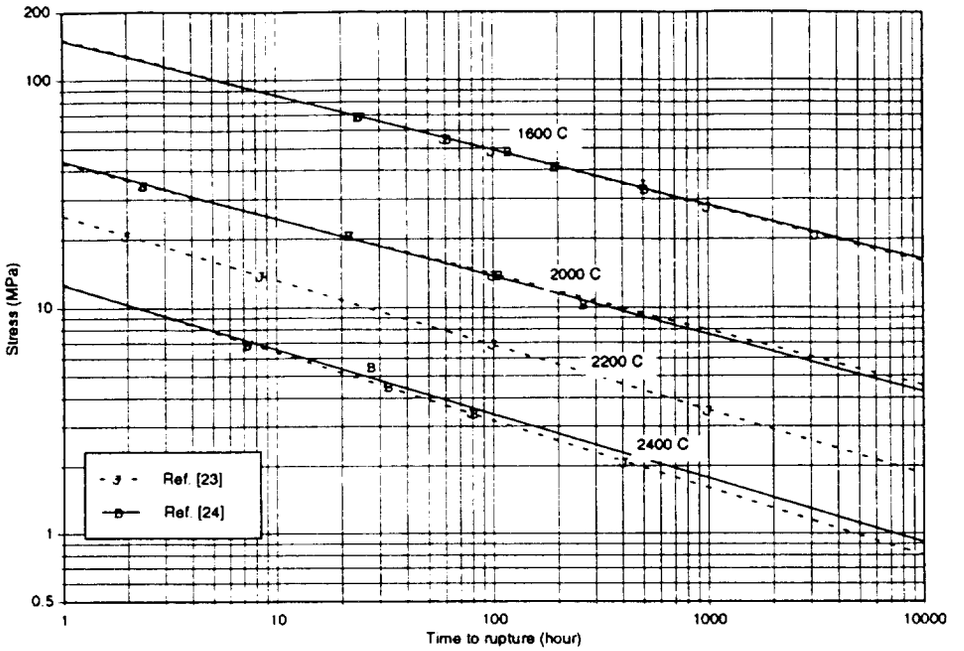

Figure 8 - *Creep-Rupture data for Arc-Cast W-Re(25) sheet tested in hydrogen [23-24].*

Nevertheless, given the high values of stresses, we must consider the creep behaviour of the material also at lower T_H in order to evaluate (1) stress relaxation, (2) possibility of creep rupture at high beam intensity and (3) window deformations and buckling[2] behaviour.

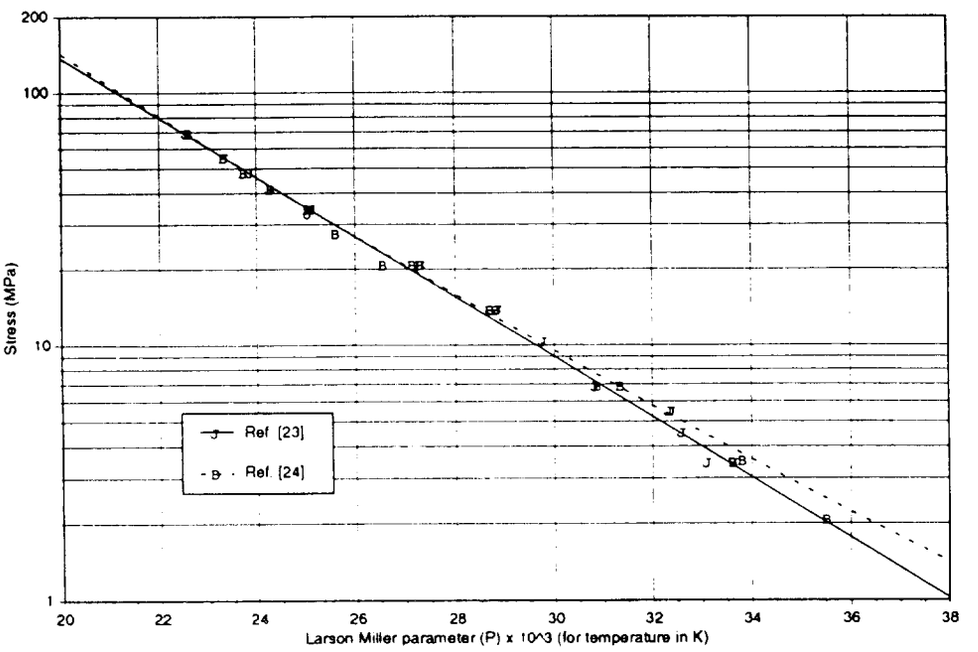

Figure 9 - *Larson-Miller parameters for Arc-Cast W-Re(25) sheet tested in hydrogen[23-24].*

[2]Buckling analysis is a technique used to determine critical loads at which a structure becomes unstable.

These evaluations are purely indicative, since based on Larson-Miller extrapolation (figure 9) of data (figure 8) at higher temperatures (1600 to 2400 °C) and lower stresses (1-100 MPa) [23-27].

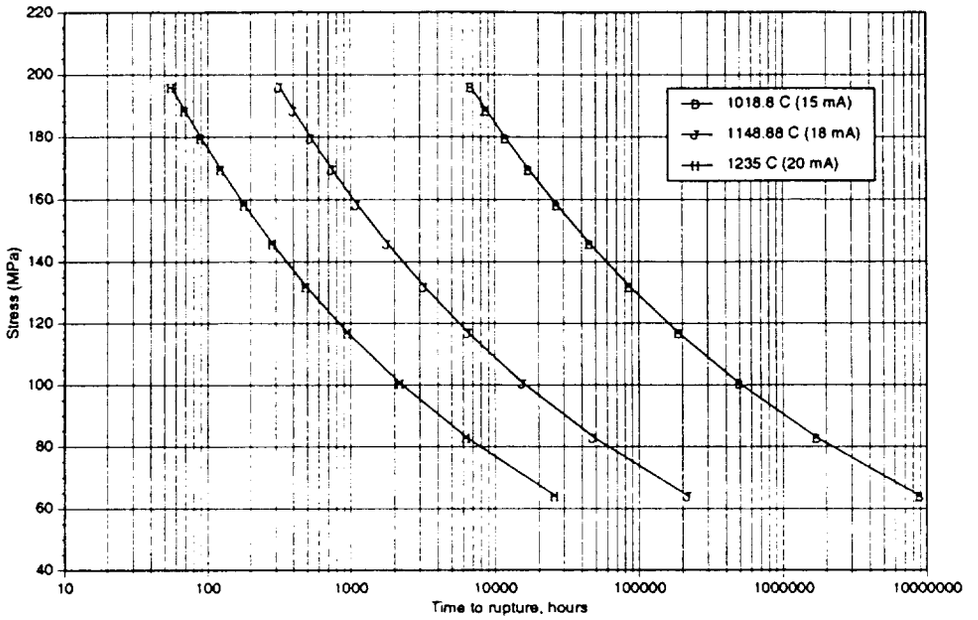

Figure 10 - *Extrapolated Stress-Rupture curves for Arc-Cast W-Re(25) sheet.*

In figure 10 we show an example of extrapolated Creep-Rupture curves for Arc-Cast W-Re(25) sheets tested in hydrogen [23,24].

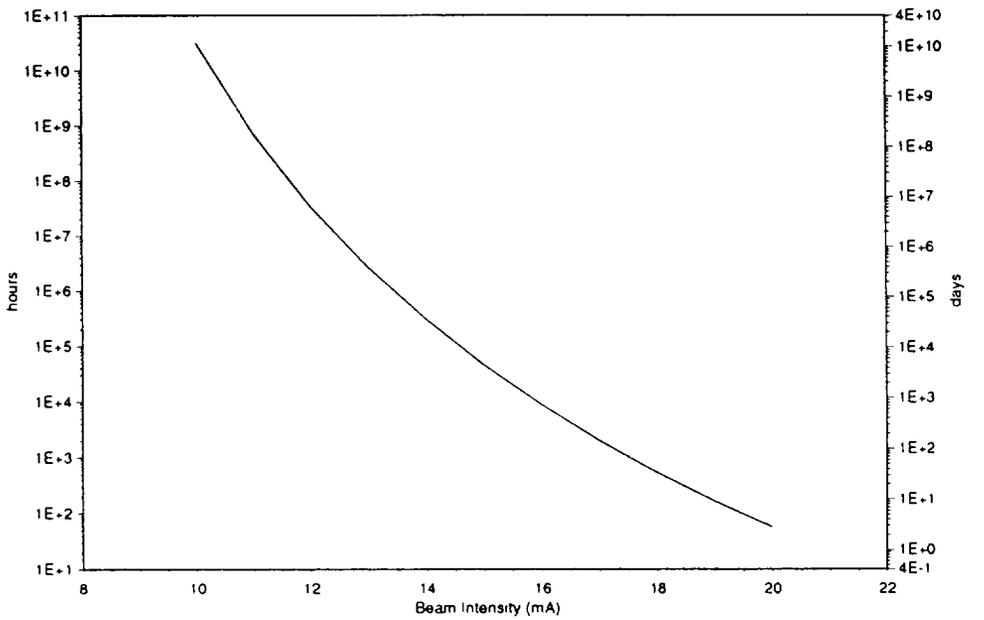

Figure 11 - *Creep-Rupture time for the Energy Amplifier beam window.*

Figure 11 shows Creep-Rupture time for the beam window, given the operating temperature and the maximum tensile stress at each beam intensity. This curve has to

be considered a low limit that is never attained, since it is based on constant stress test. In our conditions creep deformations rapidly reduce stresses, especially at high temperatures. We therefore expect sensibly longer window lifetimes.

To have an idea of stress relaxation we ran a 10000 hr, creep analysis with ANSYS at 15 mA, based on the extrapolation of creep rates contained in reference [25-27]. As showed in figure 12 (at the end of the document) the maximum tensile stress is reduced by more than a factor 3 (from 145 to 48 MPa), although deformation is negligible and the structure is stable at buckling pressures above 60 bar.

A creep analysis at 400 hr and 20 mA shows a stress reduction of about a factor 2.3 (from 233 to 101 MPa), and a more significant deformation (about 0.56 mm in the region of higher stresses) which does not introduce instability up to buckling pressures of more than 38 bar.

At high beam intensity, we therefore expect longer duration of the beam window with respect to the limit described in figure 11, but it is difficult to make a good prediction of the lifetime without further experimental data, given the time dependency of the stresses.

4.0 Conclusions

The Energy Amplifier shares the need for a reliable and robust beam window together with most of the high power spallation sources currently under study or construction in the world.

Nevertheless, the requirements for such a window in the case of the EA are more stringent, since, to enhance the passive nature of the device for safety reasons, the cooling system is only based on molten Lead natural convection , and acts only on the external surface of the window, while in most other cases a double forced cooling system is employed (see for example ref. [28,29]).

Accurate calculations based on finite element methods show that the use of a Tungsten-Rhenium (26%) refractory alloy as a beam window material for the Energy Amplifier seems feasible from a mechanical point of view, at least for beam intensities up to 17-18 mA. This limit is anyway purely indicative, since based on extrapolated data. A dedicated experimental activity, could asses it with more precision.

Important uncertainties remain concerning the radiation damage from the proton beam, since no specific and exhaustive tests have never been made on such a material (and are also poor for other different materials). Limited bibliography on radiation damage indicates that the major problem of W-Re could be neutron embrittlement, but a series of tests have to be planned in order to study the behaviour of this material under irradiation.

References

[1] *S. Buono,, C. Rubbia* "A Numerical model of the primary cooling loop of the Energy Amplifier based on Lead natural convection", CERN/AT/ET Internal Note n. 15 May 1996.

[2] *C. Rubbia et al..*, "Conceptual design of a Fast neutron operated high power Energy Amplifier", CERN/AT/95-44(ET), 29 September, 1995.

[3] "STAR-CD Version 2.3 Manuals", Computational Dynamics, 1996.

[4] *Fassó et al.*, "Intermediate Energy nuclear data: models and codes". Proceedings of a specialists' meeting at Issy les Moulinex (France) 30 May - 1 June 1994, p. 271 (published by OECD, 1994).

[5] *AA.VV.*, "ANSYS User's Manual, version 5.2", Vol I,II,III,IV, "ANSYS Structural Nonlinearities", "ANSYS Thermal Analysis", Swanson Analysis System, Inc. Huston.

[6] *M. Battistin et al.*, " A thermal structural analysis of the beam window of the Fast Energy Amplifier", CERN/AT/ET Internal Note n. 95-032, July 17, 1995.

[7] *Shunk*, "Constitution of binary alloys", Mc Graw-Hill, 1969.

[8] *J.J. Park, D.L.Jacobson*, "Creep behaviour of Tungsten - 4 Rhenium - 0.32 Hafnium Carbide", Proceedings of the First International Conference on Tungsten and Tungsten Alloys, November 15-18, 1992, Arlington, Virginia.

[9] *R.H.Tham, H. Nahme*, "Dynamic behaviour of Tungsten Rhenium alloys", Proceedings of the First International Conference on Tungsten and Tungsten Alloys, November 15-18, 1992, Arlington, Virginia.

[10] *F.J.Ritzert, R.L.Dreshfield*, "Progress toward a Tungsten alloy wire/high temperature alloy composite turbine blade", Proceedings of the First International Conference on Tungsten and Tungsten Alloys, November 15-18, 1992, Arlington, Virginia.

[11] *A. Luo, D.L. Jacobson*, "Solution softening and dispersion strengthening in Tungsten", Proceedings of the First International Conference on Tungsten and Tungsten Alloys, November 15-18, 1992, Arlington, Virginia.

[12] "Tungsten", Plansee data sheet.

[13] *B.H.Tsao, M.L.Ramalingam*, "The effect of ThO_2 and HfC on the recrystallization of W-Re alloys", Proceedings of the symposium by the Refractory Metals Committee held at the 120th annual meeting of the Minerals, Metals and Materials Society, in New Orleans, Louisiana, February 17-22, 1991.

[14] *L. Mansur*, "Spallation Radiation Effects in Materials", presentation given at the First International Workshop on the Technology and Thermal Hydraulics of Heavy Liquid Metals, Schruns, March 24-29 1996.

[15] *H. Ullmaier, F. Carsughi*, "Radiation damage problems in high power spallation neutron sources", NIM B 101 (1995) 406-421.

[16]*R. Herschits, D.N. Seidman,* "An atomic resolution study of homogeneous radiation-induced precipitation in a neutron irradiated W-10at% Re alloy", Acta Metall. 32-8 pp 1141-1154, 1984.

[17] J. Matholich, H. Nahm, J. Moteff, "Swelling in Neutron irradiated Tungsten and Tungsten-25 percent Rhenium", Scripta Metallurgica, vol. 8, pp 837-842, 1974.

[18] *T. T. Claudson,* Effects of Neutron Irradiation on the Elevated Temperature Mechanical Properties of Nickel-Base and Refractory Metal Alloys", Am. Soc. Testing Mats., 1967, pp. 67-94.

[19] *P. Krautwasser, H. Derz, E. Kny,* "Influence of fast neutron fluence on the ductile-to-brittle transition temperature of Tungsten, W-10Re and W-3.4Ni-1.6Fe", High Temperatures - High Pressures, 1990, volume 22, pages 25-32.

[20] *A. Luo, K.S. Shin, D.L. Jacobson,* "Thoria particle strengthening in W-Re 26% Alloy", Tungsten and Tungsten Alloys - Recent Advances, Edited by A. Crowson and E.S. Chen. The Minerals, Metals & Materials society, 1991.

[21] "Tungsten-Rhenium Alloys", Plansee data sheet.

[22] Goodfellow private communication.

[23] "Sixth Annual Report - High Temperature Materials Program", GE-NMPO, GEMP-475A, February 28, 1967.

[24] "AEC Fuels and Materials Development Program Progress Report No. 71", GE-NMPO, GEMP-1002, December 29, 1967.

[25] *J.B. Conway, P.N. Flagella,* "Creep-rupture data for the refractory metals to high temperatures" and references therein, Gordon and Breach Science Publishers, New York.

[26] *R.R. Vandervoort, W.L Barmore,* "Elevated Temperature Deformation and Electron Microscope Studies of Polycrystalline Tungsten and Tungsten-Rhenium Alloys", Sixth Plansee Seminar, Reutte, June 24-28, 1968.

[27] *R.R. Vandervoort,* "The creep behaviour of W-5 Re", Metallurgical Transaction, p. 857, Vol. 1, April 1970.

[28] Proceedings of the Meetings ICANS-XIII and ESS-PM4, edited by G. Bauer and R. Bercher, PSI proceedings 95-02, November 1995.

[29] Proceedings of the "First International Workshop on the Technology and Thermal Hydraulics of Heavy Liquid Metals", Schruns, March 24-29 1996.

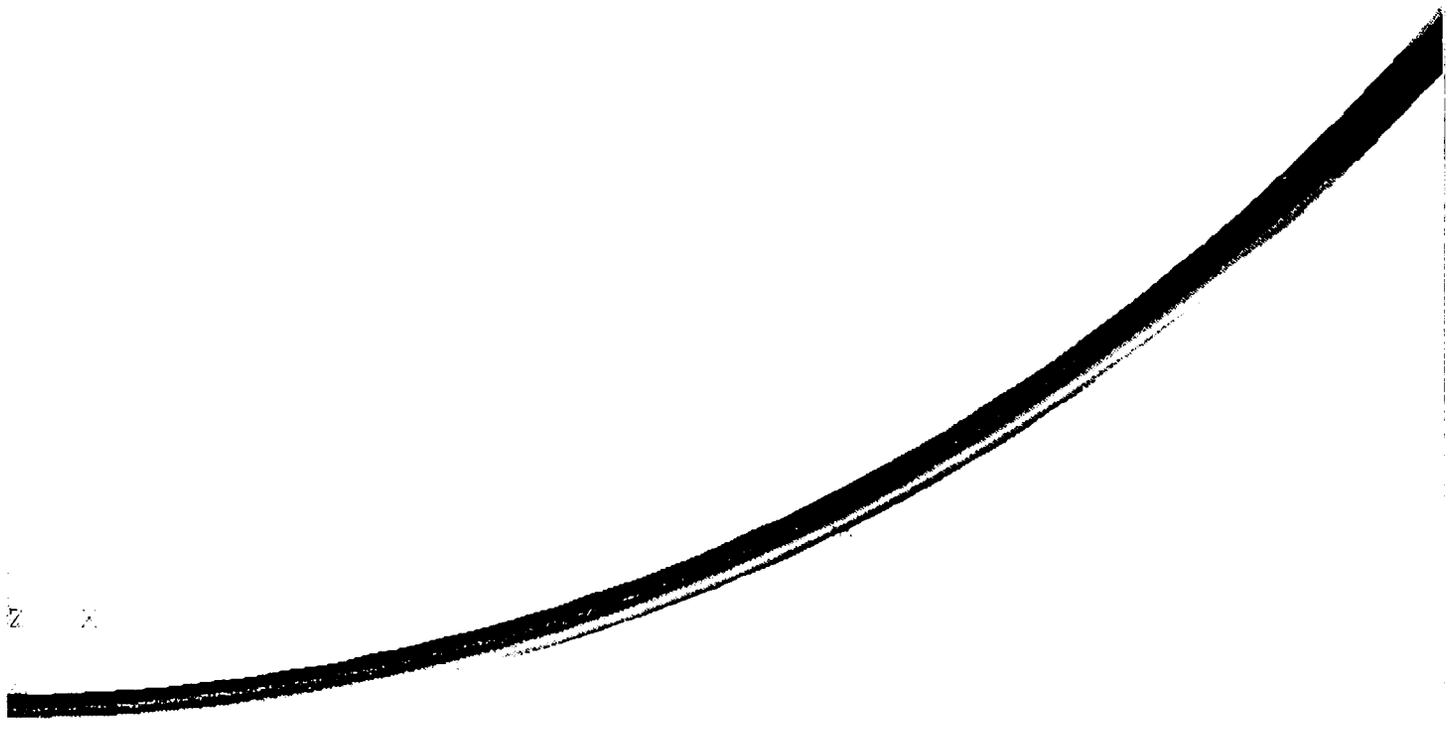

Figure 4 Parabolic stress map at 10 mA (Parabolic beam)

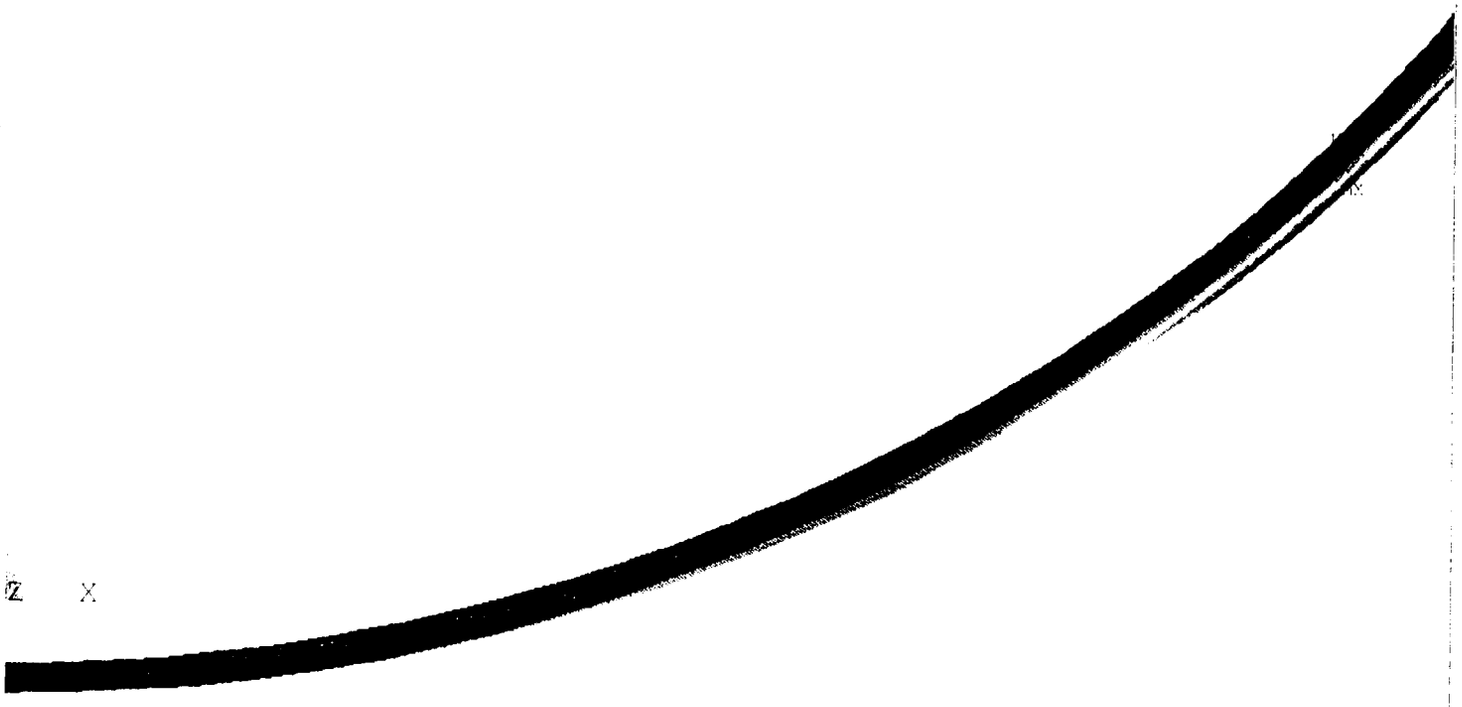

Figure 5. Tangential stress map at 10 mA (Flat beam)

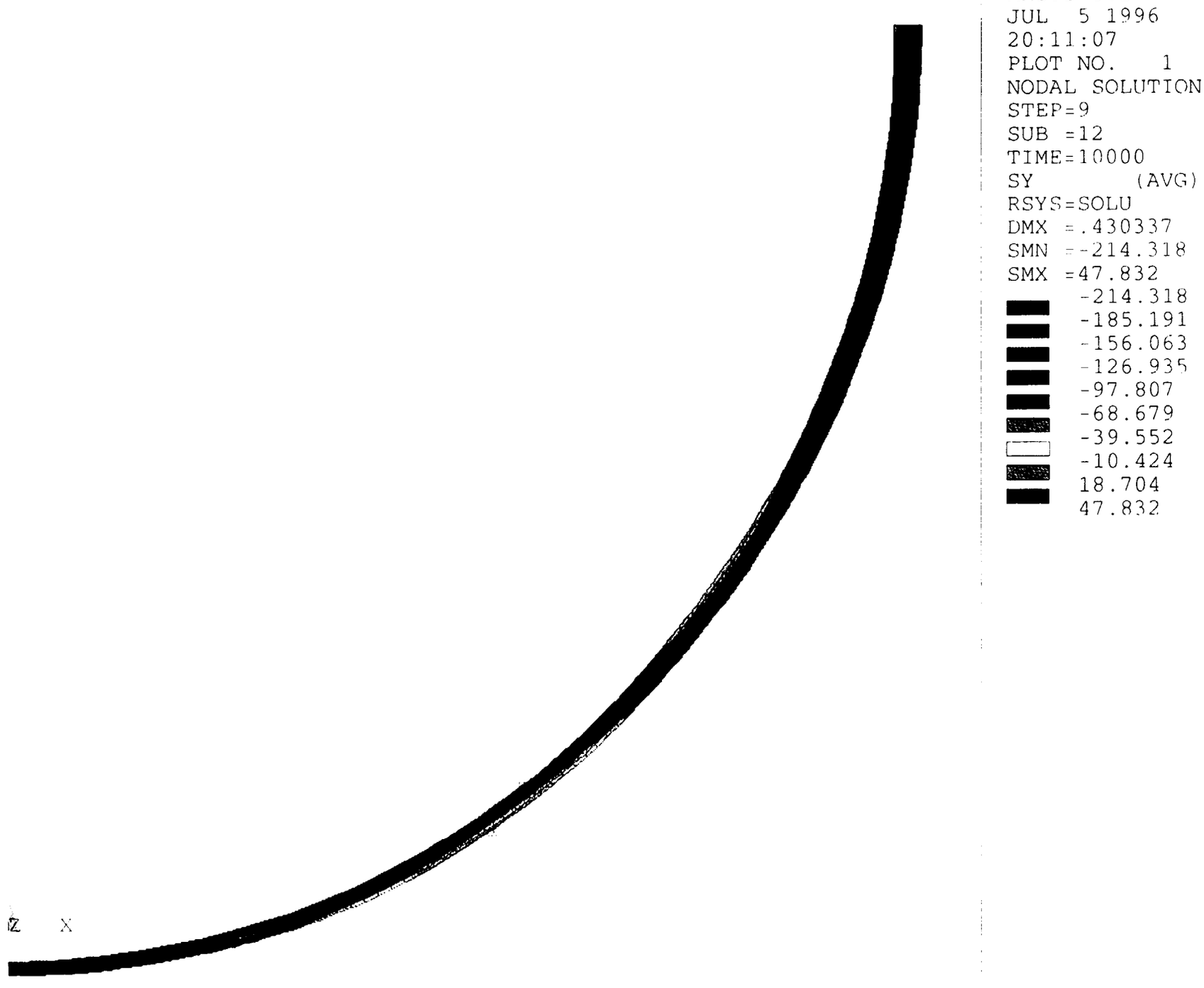

Figure 12 Stress Relaxation after 10000 hr at 15 mA